Single-electron energy subbands of a hollow cylinder in an axial magnetic field

M. Masale, N. C. Constantinou, and D. R. Tilley
Department of Physics, University of Essex, Colchester CO4 3SQ, England
(Received 20 July 1992)

The energy spectrum of a single electron confined to a hollow cylinder by an infinite square potential well is determined within the effective-mass approximation, both as a function of the radii and applied axial magnetic field. In the absence of a magnetic field, the states with nonzero azimuthal quantum number m are doubly degenerate, with the lowest-energy $m=0$ subband always the ground state. The application of an axial magnetic field lifts these degeneracies. As the field is increased, the $m<0$ subbands initially decrease in energy and attain a minimum at a magnetic field corresponding to $|m|$ elementary flux quanta (h/e) contained within the electron's cyclotron radius. The presence of the magnetic field leads to quite different conclusions regarding the nature of the ground state. For low fields, the ground state is, as before, the lowest $m=0$ state. As the field is increased, this state loses the status of being the ground state and is replaced by the lowest-energy $m=-1$ subband, which in turn is replaced by the $m=-2$ state, and so on. This behavior is due to the presence of the inner radius and is analogous to similar behavior recently predicted for a pair of interacting electrons in a solid cylinder.

I. INTRODUCTION

The behavior of electrons in the presence of a uniform magnetic field is a classic problem in quantum mechanics.[1] The advancement in nanostructure fabrication techniques, and hence the ability to confine electrons to quasi-two-dimensions, has led to a wealth of new physics, especially with the application of a magnetic field.[2,3] In particular, the physics of quasi-one- and quasi-zero-dimensional devices is now the subject of considerable attention.[4–10]

Long ago, Dingle considered the one-electron properties of small systems under the influence of a constant magnetic field, and, of relevance to this investigation, that of a solid cylinder with an axial field.[11] Perturbative techniques were employed in order to obtain the energy spectrum, together with the development of asymptotic expansions for the various special functions that arise. In an earlier paper[12] we discussed a quantum wire in an axial magnetic field. The Schrödinger equation can be solved exactly in terms of confluent hypergeometric functions,[1] so the boundary condition at the outer radius R of the wire generates an exact equation for the energy eigenvalue. The character of the solutions depends on the ratio a_c/R, where $a_c=(\hbar/eB)^{1/2}$ is the magnetic length. For $a_c/R \gg 1$ (weak field) confinement is by the cylinder alone and the energy spectrum is that of the cylinder without applied field.[13] For $a_c/R \ll 1$ confinement by the cylinder wall is irrelevant and the spectrum is the cyclotron sequence $E_n=(n+\frac{1}{2})\hbar\omega_c$ with $\omega_c=eB/\mu$, where μ is the effective mass. The lowest eigenvalue at all fields corresponds to azimuthal quantum number m equal to zero. For $B=0$, states m and $-m$ are degenerate. For small B, a linear Zeeman splitting is seen, with $E(-m)$ decreasing and $E(m)$ increasing. For large B, the quadratic coupling Hamiltonian $e^2A^2/2\mu$ is dominant with the result that both $E(-m)$ and $E(m)$ increase as B increases. This means in particular that $E(-m)$ has a minimum at an intermediate value of B.

Makar, Ahmed, and Awad[14] raised the question of the quantum mechanics of an electron in a hollow cylinder with an axial applied magnetic field. They give a discussion in terms of various limiting and asymptotic solutions, similar in spirit to the much earlier work of Dingle[11] on the solid cylinder. As for the solid cylinder, an exact solution is possible and forms the subject of this paper.

The paper is arranged as follows. In Sec. II the energy eigenvalues are discussed for the hollow cylinder in the absence of a magnetic field. Section III considers in detail the effect of an axial magnetic field on both the one-electron energies and wave functions. Some concluding remarks are contained in Sec. IV.

II. HOLLOW CYLINDER

In this section, the energy spectrum of an electron confined to a hollow cylinder of inner radius R_1 and outer radius R_2 is derived. It is convenient to work in cylindrical coordinates (ρ,φ,z). The confining potential is taken as zero in the region $R_1 \le \rho \le R_2$ and infinite otherwise. The effective-mass Schrödinger equation is separable[13] and the wave function ψ is given by

$$\psi=[PJ_m(q\rho)+QY_m(q\rho)]e^{ik_z z}e^{im\varphi}, \quad m=0,\pm1,\pm2,\ldots, \tag{2.1}$$

with

$$q^2=2\mu E_{ml}/\hbar^2 . \tag{2.2}$$

In the above P and Q are constants determined by normalization and the boundary conditions, μ the effective mass, k_z the axial wave vector, $J_m(x)$ and $Y_m(x)$ Bessel functions of order m, are as defined in Ref. 15. The subband energy E_{ml}, is related to the total energy via

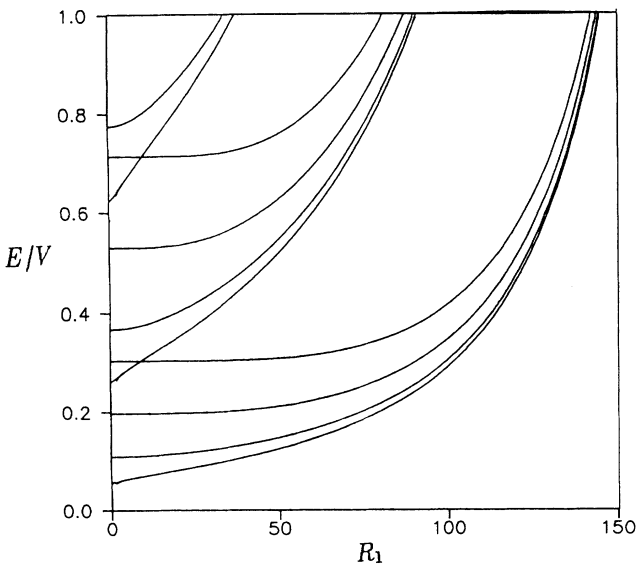

FIG. 1. Lowest-order energy eigenvalues as a function of increasing inner radius R_1 and outer radius $R_2=200$ Å. For $R_1=0$, the $(l,|m|)$ sequence is $\{(0,0),(0,1),(0,2),(1,0),(0,3),(1,1),(1,2),(2,0),(1,3),(2,1)\}$.

$$E_T=E_{ml}+\frac{\hbar^2k_z^2}{2\mu} \tag{2.3}$$

and is labeled by the azimuthal quantum number m and the radial quantum number l. The Bessel function $Y_m(x)$ is allowed in the case of a hollow cylinder, although for a solid cylinder it is discarded due to its divergent behavior at the origin.

The boundary conditions, namely, the vanishing of ψ at R_1 and R_2, lead to the following eigenvalue equation:

$$J_m(qR_1)Y_m(qR_2)-J_m(qR_2)Y_m(qR_1)=0 . \tag{2.4}$$

The above equation is solved numerically for the energy eigenvalue E_{ml}. Figure 1 depicts the lowest subbands as a function of inner radius R_1, with R_2 fixed at 200 Å. The energy scale is in units of V ($\approx$190 meV), the conduction-band offset between GaAs and $Al_{0.25}Ga_{0.75}As$, and the curves are labeled by their quantum numbers (l,m). It should be noted that the subband (0,0) remains the ground state whatever the inner radius, and that states with nonzero azimuthal quantum number are doubly degenerate ($E_{ml}=E_{-ml}$). For small inner radius, there is an appreciable separation between states corresponding to different m but equal l quantum numbers. As R_1 approaches R_2, the states with equal l values converge, with their energies having an $(R_2-R_1)^{-2}$ variation.

III. APPLIED MAGNETIC FIELD

Application of a constant axial magnetic field is known to dramatically alter the energy spectrum in the case of a solid cylinder.[12] In this section analytical results are presented for the case of a hollow cylinder under the influence of a constant axial magnetic field B. Although the procedure leading to the solution of Schrödinger's equation follows the same path as that described for the solid cylinder, the results obtained are qualitatively and quantitatively different.

It is convenient to work in the Landau and Lifshitz gauge[1] for the vector potential $\mathbf{A}$:

$$\mathbf{A}=(0,\tfrac{1}{2}B\rho,0) . \tag{3.1}$$

In the above gauge, the Hamiltonian for an electron with charge $-e$ is

$$\hat{H}=(\hat{p}_\rho^2+\hat{p}_z^2)/2\mu+(\hat{p}_\phi+\tfrac{1}{2}eB\rho)^2/2\mu , \tag{3.2}$$

where $\hat{p}=-i\hbar\nabla$ is the momentum operator. Again, as in the preceding section, the effective-mass Schrödinger equation is separable, with the details given in our previous work.[12] The wave function may now be written as

$$\psi=\xi^{|m|/2}\exp(-\xi/2)[\tilde{P}M(a,b,\xi)+\tilde{Q}U(a,b,\xi)] \times e^{ik_zz}e^{im\varphi} , \tag{3.3}$$

with $\tilde{P}$ and $\tilde{Q}$ constants determined via the normalization and the boundary conditions.

In Eq. (3.3), a and b are parameters given by

$$a=\tfrac{1}{2}(1+|m|+m)-E_{ml}/\hbar\omega_c \tag{3.4}$$

and

$$b=|m|+1 , \tag{3.5}$$

with ξ a dimensionless variable defined as

$$\xi=\rho^2/2a_c^2 . \tag{3.6}$$

The functions $M(a,b,\xi)$ and $U(a,b,\xi)$ are the confluent hypergeometric functions,[15] and, since the cylinder is hollow, $U(a,b,\xi)$ is an allowed solution. For the solid cylinder, $U(a,b,\xi)$ is divergent at the origin.

The following dispersion relation follows from the application of the boundary conditions:

$$M(a,b,R_1^2/2a_c^2)U(a,b,R_2^2/2a_c^2) -M(a,b,R_2^2/2a_c^2)U(a,b,R_1^2/2a_c^2)=0 . \tag{3.7}$$

Equation (3.7) may be solved numerically by employing the recursion relations satisfied by the confluent hypergeometric functions together with their integral representations. These are outlined in Appendix A. Figures 2(a) and 2(b) show examples of the magnetic field dependence of the subbands for $l=0$ and different m values. In Fig. 2(a) the inner radius is 50 Å, while in Fig. 2(b) the inner radius is 200 Å, with $R_2=300$ Å for both. As in the case of the solid cylinder, the $|m|\neq0$ states, which are doubly degenerate in the absence of a field, are split and show a linear Zeeman splitting for small B and a linear increase for large magnetic field. In consequence, the negative m states pass through a minimum at a value of B given by

$$\pi\langle\rho^2\rangle B=|m|\Phi_0, \quad m=-1,-2,-3,\ldots , \tag{3.8}$$

where $\Phi_0(=h/e)$ is the elementary flux quantum and $\langle\rho^2\rangle$ is the expectation value of ρ^2. Table I lists the

values of B, $\langle \rho^2 \rangle$, and $\pi\langle \rho^2 \rangle B/\Phi_0$ at the minima of Fig. 2(b), the value of $\langle \rho^2 \rangle$ being evaluated numerically using the normalized wave functions. It is seen that to an excellent approximation, (3.8) is satisfied. In fact, a simple semiclassical argument may be invoked to derive (3.8) and this is outlined in Appendix B.

Just as with the solid cylinder, the minimum for the $m<0$ states occurs when $|m|$ flux quanta are contained within the electron's cyclotron radius. There is, however, an important and striking difference between the hollow and solid cylinders. For the latter, the ground state is always (0,0). For the hollow cylinder, however, (0,0) is the lowest subband at low fields, but at higher fields is replaced by $(0,-1)$ which in turn is replaced by $(0,-2)$ as

TABLE I. Values of the minimum B, $\langle \rho^2 \rangle$, and $\pi\langle \rho^2 \rangle B/\Phi_0$ corresponding to Fig. 2(b).

B (T)	$\langle \rho^2 \rangle / R_2^2$	$\pi\langle \rho^2 \rangle B/\Phi_0$
2.10	0.70	1.00
4.15	0.70	1.98
6.30	0.70	3.00
8.35	0.70	3.99
10.45	0.70	4.99
12.55	0.70	5.99

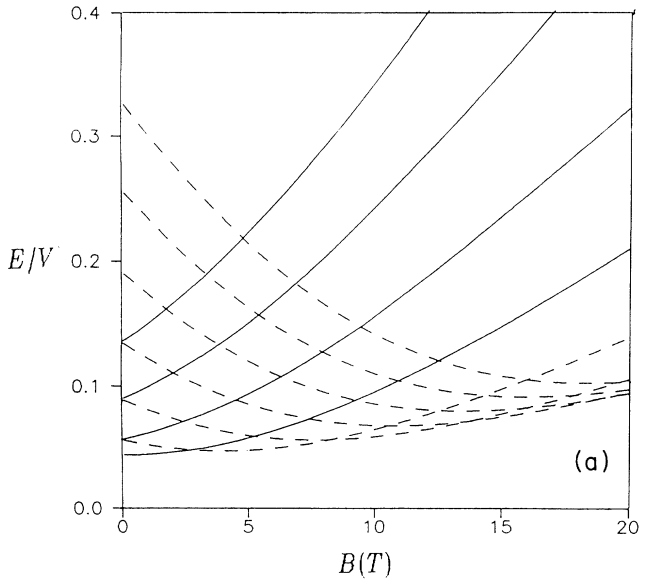

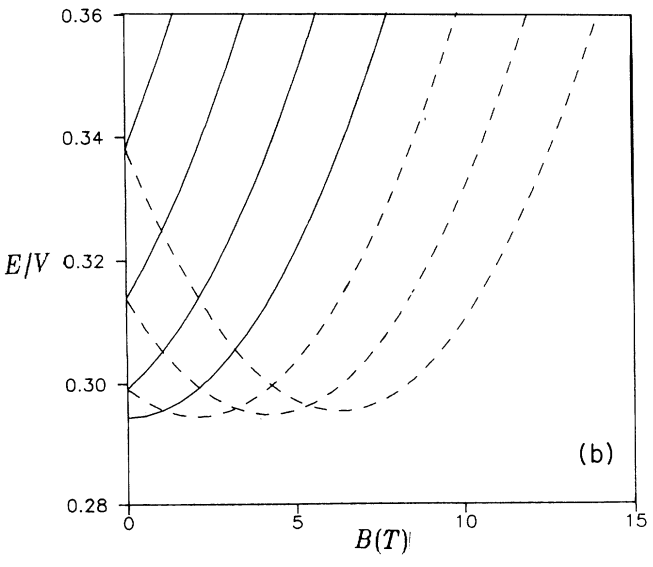

FIG. 2. The $l=0$ subband energies as a function of axial field B for (a) $R_1=50$ Å and (b) $R_1=200$ Å with $R_2=300$ Å in both cases. The dashed curves correspond to $m<0$ and the solid curves to $m\geq 0$. At $B=0$ the $|m|$ values are (a) 0–6, (b) 0–3.

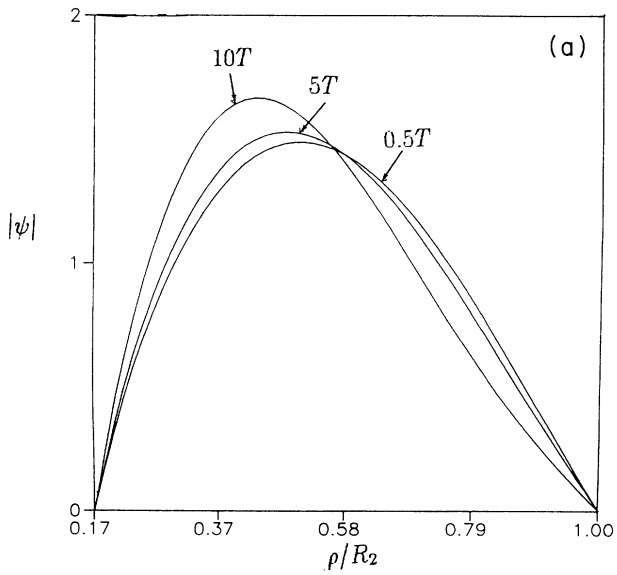

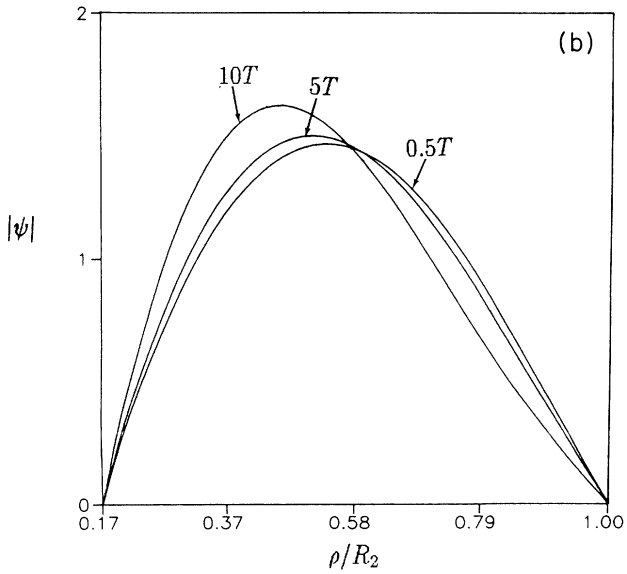

FIG. 3. Normalized radial $l=0$ wave functions for $R_1=50$ Å, $R_2=300$ Å with (a) $m=0$ and (b) $m=-1$. The values of the applied magnetic field are as indicated.

the field increases further, and so on. This is solely the result of having an inner radius R_1, which acts as a lower bound for the cyclotron radius. As the magnetic field is increased, the (0,0) wave function, as is demonstrated later, is "squeezed" towards the inner wall, and hence its energy increases rapidly. Hence the $(0,-1)$ state becomes the ground state. It is interesting that qualitatively similar features are predicted for a solid cylinder containing two interacting electrons.[10] Here the two-particle wave function has a zero on the axis due to the Coulomb repulsion. This is analogous to the forbidden region in the one-electron system considered here ($\rho < R_1$). The successive substitution of the ground state occurs at lower magnetic fields for Fig. 2(b), ($R_1 = 200$ Å), compared to Fig. 2(a) where $R_1 = 50$ Å due to the larger inner radius of the former.

It should be emphasized here that these minima in the energies occur in systems with spherical symmetry also. In fact, Praddaude[16] predicted minima in the negative m states for hydrogenlike atoms in an intense magnetic field.

To conclude this section, the effect of an axial magnetic field on the wave functions is considered for the various states of a hollow cylinder which corresponds to the subband spectrum depicted in Fig. 2(a). Figures 3(a) and 3(b) show the effect of the axial magnetic field ($B = 0.5$, 5, and 10 T) on the lowest-energy $m = 0$ and -1 states, respectively. As expected on physical grounds the wave-function peak shifts towards the inner radius of the cylinder as the field is increased, hence the increase in the energy.

Figures 4(a) and 4(b) show the $l = 0$ radial wave functions corresponding to the different azimuthal quantum numbers ($|m| = 0, 1, 2, 3$) for low magnetic fields ($B = 0.5$ T) and for a higher magnetic field ($B = 10$ T), respectively. The wave-function peak shifts away from the inner radius, towards the center of the cylindrical shell as $|m|$ increases due to the increase in the angular momentum. Clearly, for a given magnetic field, the lowest nonzero m can be found for which the cyclotron radius of the electron is the allowed quantized semiclassical orbit. The corresponding energy subband, in reference to Fig. 2(b), will consequently become the ground state.

Figure 5 illustrates some higher-order wave functions having azimuthal quantum number $m = 2$ for $B = 10$ T. The radial quantum number is essentially a count of the

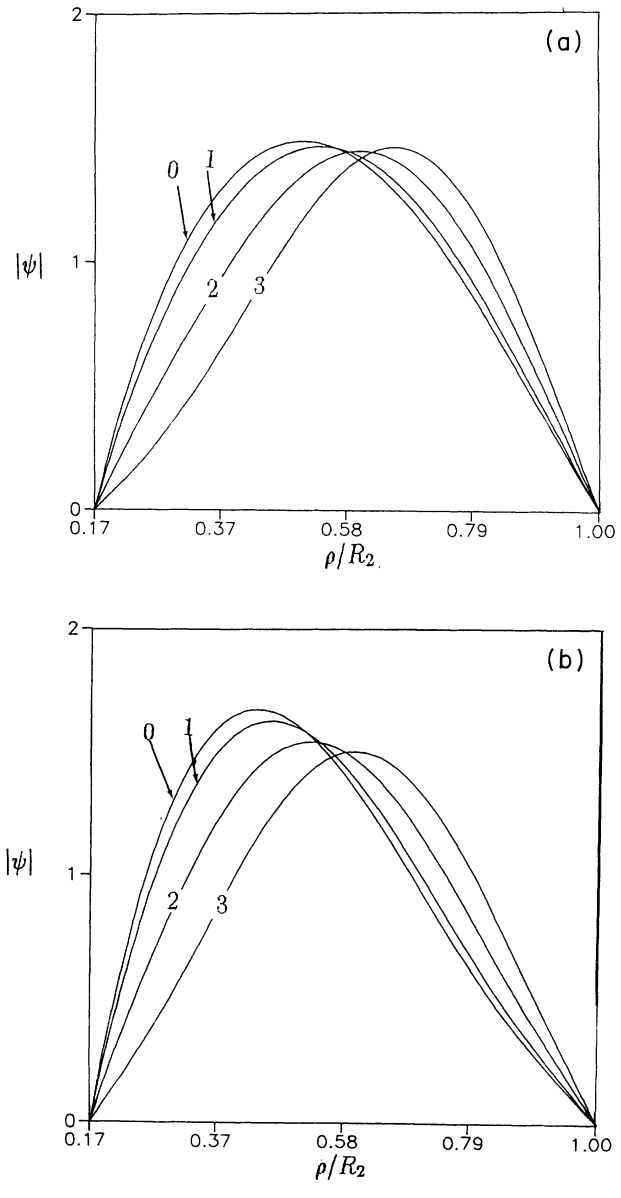

FIG. 4. Normalized $l = 0$ radial wave functions for $R_1 = 50$ Å and $R_2 = 300$ Å at different constant applied magnetic fields (a) $B = 0.5$ T; (b) $B = 10$ T, showing the wave-function peak shift away from the inner radius with increasing $|m| = 0$, 1, 2, and 3 (as indicated).

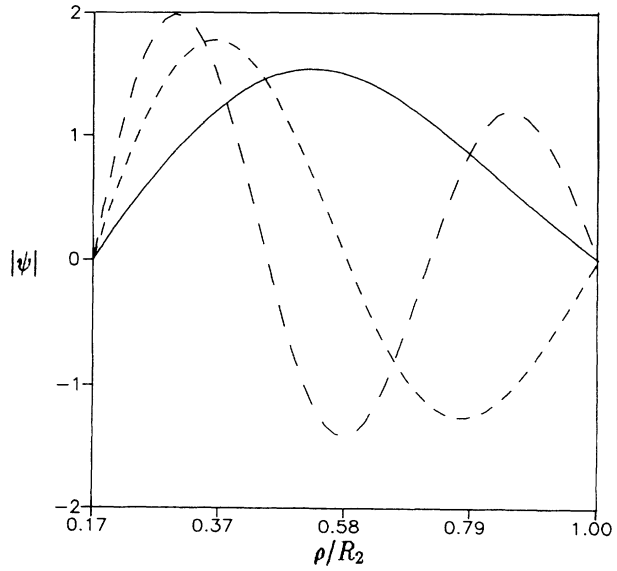

FIG. 5. Normalized $m = -2$ radial wave functions corresponding to the different radial quantum numbers $l = 0$ (full curve); $l = 1$ (small dash), and $l = 2$ (large dash). The other parameters are $R_1 = 50$ Å, $R_2 = 300$ Å, and $B = 10$ T.

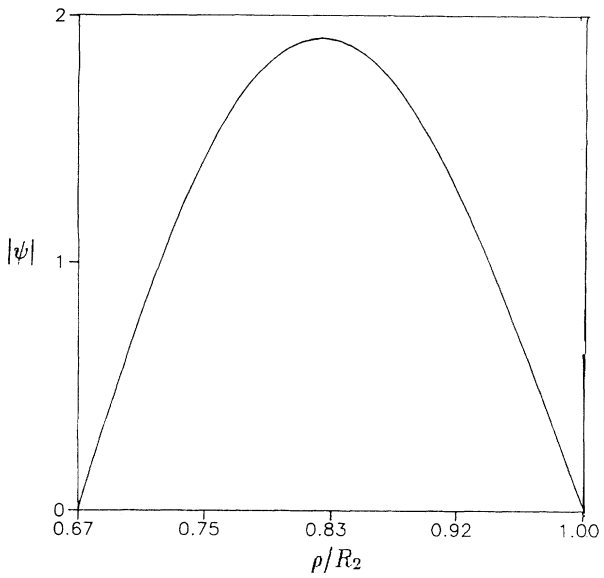

FIG. 6. Normalized lowest subband radial wave function for $R_1=200$ Å, $R_2=300$ Å corresponding to the range of B and m values ($B\leq 6$ T and $|m|\leq 3$) for which confinement of the electron is mainly by the cylindrical shell walls, and not the (low) magnetic field.

number of nodes the wave function has. Finally, Fig. 6 shows the lowest subband wave function corresponding to Fig. 2(b) ($R_1=200$ Å; $R_2=300$ Å) for a magnetic field $B=0.5$ T. For this pair of radii, confinement is mainly by the cylindrical shell walls and the wave function shows no dependence on either moderate values of B (≤ 6 T) or moderate m ($|m|\leq 3$).

IV. CONCLUSIONS

Analytic solutions of the one-electron effective-mass Schrödinger equation have been presented for a hollow cylinder. The energy spectrum was investigated both without and with an applied constant axial magnetic field. In the absence of a magnetic field, the lowest-energy $m=0$ subband is always the ground state whatever the values of the radii. This is also true for the solid cylinder and remains true for the solid cylinder even with an axial magnetic field.[12] The application of an axial magnetic field to a hollow cylinder leads to a drastic modification in the subband spectrum. In particular, there is a succession of ground states corresponding to $m=0,-1,-2,\ldots$ as the field is increased, although the radial quantum number remains zero. This behavior is analogous to that predicted for two electrons in a solid cylinder interacting via their Coulomb potential. Furthermore, just as with the solid cylinder, the negative m states have a minimum in their variation with magnetic field at a field corresponding to $|m|$ flux quanta contained within the cyclotron radius.

An extensive list of recent experimental references is given in our previous publication.[12] In particular, the recent investigation by Patel *et al.*[17] in which an in-plane magnetic field is applied to a one-dimensional constriction is the most relevant.

ACKNOWLEDGMENTS

M.M. thanks the University of Botswana and N.C.C. thanks the United Kingdom Science and Engineering Research Council for financial support.

APPENDIX A

This is a brief comment on how the confluent hypergeometric functions were evaluated since they are not available in standard libraries. The strategy adopted in evaluating these functions is the same for both. It is therefore sufficient to consider only one of them, U, say. In the notation of Ref. 15,

$$U(a,b,z)=\frac{1}{\Gamma(a)}\int_0^\infty e^{-zt}t^{a-1}(1+t)^{b-a-1}dt \quad \text{(A1)}$$

subject to the constraint that $a>0$; $z>0$. The parameter given by Eq. (3.4), however, is negative for a wide range of magnetic fields. In order to satisfy the condition that $a>0$, the following recursion was used iteratively on itself:

$$U(a,b,z)+[b-z-2(a+1)]U(a+1,b,z)+(a+1)(2+a-b)U(a+2,b,z)=0 . \quad \text{(A2)}$$

Now, after $j\geq|a|$ iterations, the equation for U becomes

$$U(a,b,z)=\alpha_j U(a+1+j,b,z)+\beta_j U(a+2+j,b,z) , \quad \text{(A3)}$$

where α_j and β_j are factors accumulated from the use of the recursion relation j times. Once the necessary number of iterations has been made, the integral representation for U, Eq. (A1), can then be applied as follows:

$$U(a,b,z)=\frac{\alpha_j}{\Gamma(a+1+j)}\int_0^\infty e^{-zt}t^{a+j}(1+t)^{b-a-j-2}dt+\frac{\beta_j}{\Gamma(a+2+j)}\int_0^\infty e^{-zt}t^{a+j+1}\times(1+t)^{b-a-j-3}dt . \quad \text{(A4)}$$

For purposes of the numerical work carried out here, $\Gamma(a)U(a,b,z)$ was calculated rather than $U(a,b,z)$ itself. Such a procedure only modifies the factors multiplying the integrals.

The $M(a,b,z)$ function can be evaluated in exactly the same way as above, but is subject to the condition $b>a>0$. A suitable recursion then is one that increments both a and b provided that $|a|$ is not too large in which case it may be necessary to use more than one recursion relation. The series representation for the M function is useful when the a parameter is negative and in particular for small argument, z, since convergence is then fast and good accuracy can be reached by taking a reasonably small number of terms.

APPENDIX B

Here a semiclassical derivation of Eq. (3.8) is outlined in a simple way. An electron with charge $-e$ is constrained to move on a plane with a magnetic field B in the $\hat{z}$ direction perpendicular to the plane. The canonical momentum $\mathbf{p}$ is

$$\mathbf{p}=\mu\mathbf{v}+e\,\mathbf{A}\ , \tag{B1}$$

where $\mathbf{v}$ is the velocity and $\mathbf{A}$ the vector potential which is given by Eq. (3.1). For an electron with negative azimuthal quantum number the velocity and the vector potential lie in opposite directions, hence

$$p_{\varphi}=-\mu v+\tfrac{1}{2}eB\rho=-\tfrac{1}{2}\rho eB\ . \tag{B2}$$

The angular momentum $\mathbf{J}$ is then simply

$$\mathbf{J}=-\tfrac{1}{2}\rho^2 eB\hat{\mathbf{z}}\ . \tag{B3}$$

From the correspondence principle, the magnitude of the angular momentum is a multiple of $\hbar$ for large quantum numbers, viz.,

$$e\pi\rho^2 B=|m|h,\quad m=0,-1,-2,-3\ . \tag{B4}$$

Equation (B4) is the semiclassical analog to (3.8) and just describes the quantized orbits of a classical electron in a magnetic field. Equation (B4) is exact for large quantum numbers.

It is worth pursuing the argument further by considering a thin cylindrical shell $R_1\simeq R_2=R$. Then, from Eq. (B4) the allowed cyclotron radius for a given m decreases as B increases. The ground state is then determined by the m value which corresponds to the orbit closest to R_2. This gives a semiclassical description of the successive ground states as a function of B discussed in the text. Furthermore, within this semiclassical framework, the energies at these minima are given by

$$E_{\min}=|m|\hbar\omega_c=\frac{R^2e^2B^2}{2\mu}\ . \tag{B5}$$

Figure 7 illustrates the variation of the minimum energy of the various $m<0$ states as a function of magnetic field using the full quantum-mechanical calculation described in the text for $R_1=200$ Å and $R_2=300$ Å. It is seen that variation of $E_{\min}$ with B follows Eq. (B5) to a good approximation, even for small m values.

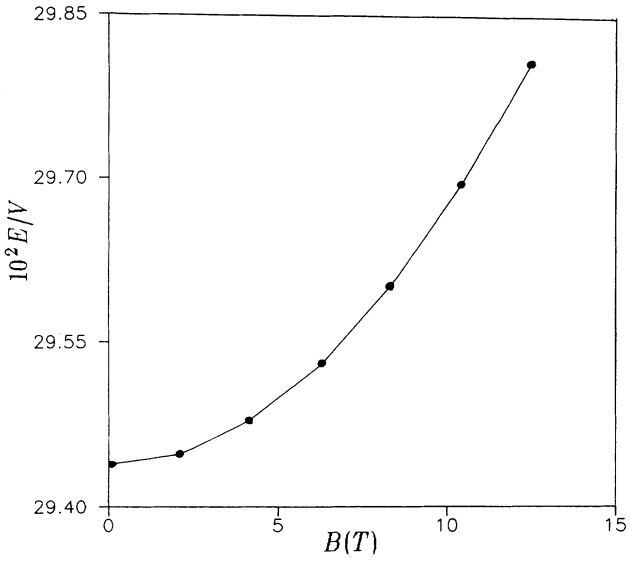

FIG. 7. Variation of the minimum energies (dots) as a function of B (the lines are a guide to the eye). The lowest energy corresponds to $m=0$, then $m=-1$, and so on.

[1] L. D. Landau and E. M. Lifshitz, *Quantum Mechanics* (Pergamon, Oxford, 1985).

[2] T. Ando, A. B. Fowler, and F. Stern, Rev. Mod. Phys. **54**, 437 (1982).

[3] M. J. Kelly and R. J. Nicholas, Rep. Prog. Phys. **48**, 1699 (1985).

[4] T. J. Thornton, M. Pepper, H. Ahmed, D. Andrews, and G. J. Davies, Phys. Rev. Lett. **56**, 1198 (1986).

[5] A. S. Plaut, H. Lage, P. Grambow, D. Heitmann, K. von Klitzing, and K. Ploog, Phys. Rev. Lett. **67**, 1642 (1991).

[6] *Science and Engineering of One and Zero Dimensional Semiconductors,* Vol. 214 of *NATO Advanced Study Institute, Series B: Physics,* edited by S. P. Beaumont and C. M. Sotomayor Torres (Plenum, New York, 1990).

[7] A. Kumar, S. E. Laux, and F. Stern, Phys. Rev. B **42**, 5166 (1990).

[8] P. A. Maksym and T. Chakraborty, Phys. Rev. Lett. **65**, 108 (1990).

[9] U. Merkt, J. Huser, and M. Wagner, Phys. Rev. B **34**, 7320 (1991)

[10] M. Wagner, U. Merkt, and A. V. Chaplik, Phys. Rev. B **45**, 1951 (1992).

[11] R. B. Dingle, Proc. R. Soc. London, Ser. A **212**, 47 (1952).

[12] N. C. Constantinou, M. Masale, and D. R. Tilley, J. Phys. Condens. Matter **4**, 4499 (1992).

[13] N. C. Constantinou and B. K. Ridley, J. Phys. Condens. Matter **1**, 2283 (1989).

[14] M. N. Makar, M. A. Ahmed, and M. Awad, Phys. Status Solidi B **167**, 647 (1991).

[15] *Handbook of Mathematical Functions,* edited by M. Abramowitz and I. Stegun (Dover, New York, 1965).

[16] H. C. Praddaude, Phys. Rev. A **6**, 1321 (1972).

[17] N. K. Patel, J. T. Nicholls, L. Martin-Moreno, M. Pepper, J. E. F. Frost, D. A. Ritchie, and G. A. C. Jones, Phys. Rev. B **44**, 10 973 (1991).